Application of direct laser marking of products made of different types of alloys using ultra-dense matrix nanobar-code

E. I. Pryakhin, *Dr. Eng., Prof., Head of the Dept. of Materials Science and Technology of Art Products* [1], *e-mail: e.p.mazernbc@yandex.ru;*
A. Yu. Dranova, *Postgraduate Student, Dept. of Materials Science and Technology of Art Products* [1], *e-mail: alinadron98@gmail.com*

[1] *Empress Catherine II Saint Petersburg Mining University (St. Petersburg, Russia)*

This paper presents a study of the influence of laser parameters (power and speed) on image contrast when applying markings using an ultra-dense nanobar-code on metal surfaces made of different materials. The experiment was conducted using a MiniMarker-2 laser system. A mode matrix was constructed by varying the parameters. The article examines the technology of laser application of an ultra-dense matrix nanobar-code (NBC) with a module size of 50-100 µm, designed for product identification in the context of Industry 4.0 concepts. Unlike traditional QR and DataMatrix codes, NBC provides high information density in an area of less than 1 mm^2. A systematic comparative study was conducted on four materials with fundamentally different physical and chemical properties: stainless steels, titanium, brass and aluminum. The key element was the mode matrix (507 combinations of power and speed). Each mode was evaluated for contrast using RGB analysis. A 3D response surface model (Python) was constructed using the matrix, visualizing the nonlinear dependence of contrast on parameters. A two-factor experimental design with high variation resolution was also implemented using the Mini-Marker-2 laser system. It was found that maximum contrast on 08Kh13 steel is achieved not with extreme parameters, but with balanced parameters. A two-stage encoding method—forming dark and light modules using different laser modes—for artificial contrast enhancement without ablation was proposed and experimentally validated. The paper includes tables for selecting optimal laser modes, as well as photographs of the results of applying the selected modes to the surfaces of stainless steel, brass, aluminum, and titanium samples.
Key words: nanobar-code, laser marking, contrast ratio, Industry 4.0, laser radiation, matrix code, marking.
DOI: 10.17580/cisisr.2025.02.15

Identification of products becomes a decisive factor in the technological chain in the conditions of global digitalization of industrial processes and realization of Industry 4.0 concepts [1–3]. Lack or damage of marking on components can lead to violation of logistics, decrease of safety during operation risk of falsifications and problems in control at all stages of a component lifecycle [4, 5]. In this connection, information coding and technologically optimal application of identifiers on the surface of products become key factors of their high–quality marking [6, 7].

Laser marking occupies the leading positions among the existing technologies owing to their advantages:

– non-destructive contactless method of application [8];
– high resolution [9];
– absence of auxiliary consuming materials [10];
– resistance to extremal effects (mechanical, thermal, chemical) [11];
– possibility of automation of production lines [12, 13].

At present time, conventional kinds of 2D matrix codes (DataMatrix and QR codes) are used actively; they provide information capacity with high resolution of module size 250–1,000 µm, what restricts possibility of their record with use of large information volume [9, 14]. It makes them unacceptable for marking products in several industries, where record using codes with large information volume is required (what is possible only with use of codes with more dense information recording, e.g. with module size 50–100 µm. Respectively, it requires principal variations in approach to the conditions of obtaining such ultra-dense codes in laser marking of machine-building products [15].

Use of nanobar-code (NBC), the 2D matrix code with above-pointed module size, which allows locating of volumetric data on a relatively small square (**Fig. 1**), is considered as one of the prospective solutions in this direction. Such marking technology opens possibility for individual identification and protection from falsifications on the level which is inaccessible for conventional methods [16].

Fig. 1. Illustration of NBC record

© E. I. Pryakhin, A. Yu. Dranova, 2025

Previously the authors have developed the technique for determination of optimal technological parameters of NBC forming on the surface of steel 08Kh13 using the Mini-Marker-2 laser system [17]. Based on the five-factor experiment, a linear regression model was built; it connects marking contrast with laser parameters, what allowed to determine the area of optimal conditions for obtaining contrast image of nanobar-code for this steel.

This work constitutes expansion of the researches applied to four various groups of the alloys, which are most widely used in the industry: steels (stainless steels 08Kh13 – an analogue of AISI 316L, 12Kh17, 03Kh17N14M3), titanium (VT1), brass (L59) and aluminium (AMg). Selection of the above-mentioned groups was based on the idea that principally various values of laser parameters should be used for each of them in order to obtain the optimal contrast nanobar image. Each of these groups is characterized by special features – reflection coefficient, heat conductivity, oxidizing sensitivity, structural and phase compositions, what stipulates necessity of their taking into account during searching optimal parameters of laser marking [18–20].

Based on this, the aim of this work is searching the optimal parameters of laser marking for each of these four groups of alloys, using ultra-dense matrix nanobar-code, which allow providing of contrast application and reliable information scanning for these alloys.

The following tasks should be solved for reaching the formulated aim:

1. Conduction of a multi-factor experiment for determination of optimal marking procedures for each of the selected materials;
2. Analysis of relationship between contrast and technological parameters (intensity, speed, frequency, impulse duration);
3. Establishment of parameters of dual-stage marking forming (dark and light elements) for increase of optical contrast;
4. Optimization of marking speed and minimization of marking time;
5. Formulation of the scientifically substantiated managing system for parameters, which is adapted for various mechanisms and units.

Especial attention was paid to putting this technology into practice at a real industrial equipment. Based on the conducted analysis of the technical literature data it was established that combined use of laser procedures allows marking application with high contrast even on the materials with low reacting coefficient (such as aluminium) and with sensitivity to non-stable coloring (such as brass).

Materials and methods

The following materials were selected as the objects for research:

– stainless steels 08Kh13 and 03Kh17N14M3 (analogues of AISI 316L), 12Kh17 (AISI 430);

– non-ferrous metals (titanium, brass, aluminium).

The plates have width 50 mm and length 100 mm, with thickness 1.0–1.5 mm. Preliminary laser grinding with removal of micro-inequalities allowed not to take into account surface roughness of plates before marking in this research.

Selection of materials was stipulated by their wide use in different industries [21–23] and their significant features in physical and chemical properties, that provide effect on interaction with laser radiation (**Table 1**).

All above-mentioned steels and metals are widely used in instrument manufacture, agriculture, medicine, power engineering and oil and gas industry [14, 20, 24–26].

Results and discussion

Marking was conducted using the Mini-Marker-2 laser system with wave length 1064 nm, maximal intensity 30 Wt, impulse duration up to 20 ns, speed up to 32 m/s and impulse feed frequency up to 1,000 Hz [19, 27, 28].

Five-factor experiment, including examination of the ultimate values of all parameters of laser system was used in the previous work [17] for determination of the optimal conditions. It was established after evaluation of regression coefficients that high levels of intensity, frequency and impulse duration, as well as low level of marking speed were recommended to be used for maximal response – maximal marking contrast. It was revealed during testing that laser radiation frequency 40 KHz provides stability of operating parameters, as well as absence of compensating variations from the side of laser managing system, while optimal balance between peak intensity and impulse energy is achieved for impulse duration 20 ns and dark trace with distinct boundaries is forming. When varying these parameters, instability of peak intensity is observed, what decreases process reproducibility [14].

The optimal number of lines in mm lineature was determined in the same way. Linear density war identified for

Table 1. Physical and operating properties of selected materials

Material	Grade	Colour	Marking features
Stainless steel	08Kh13	Silver gray	Good contrast, stable oxidizing, suitable for marking without preliminary preparation
Stainless steel	12Kh17	Silver gray	High heat-resistance, coloured interference during overheating
Stainless steel	03Kh17N14M3	Light gray, metallic appearance	Austenite structure, sensitivity to interferential coloring, high corrosion resistance
Titanium	VT1-0	Silver gray, dim	Distinctly expressed coloured marking
Brass	L59	Golden yellow	Selective zinc evaporation, heterogeneous oxidation
Aluminium	AMg	Light gray	High reflection and heat conductivity

Table 2. Factors of laser effect and their limits

Factor		Factor variation level			
		Minimal		Maximal	
Title	Designation	number	code	number	code
Impulse intensity (Factor x_1)	P, Wt	1	–1	99	+1
Marking speed (Factor x_2)	S, m/s	1	–1	32	+1
Laser radiation frequency (Factor x_3)	F, N	const 40			
Impulse duration (Factor x_4)	τ, ns	const 20			
Number of lines per mm (Factor x_5)	μ, pieces	const 20			

Table 3. The matrix of a two-factor experiment

No. of experiment	x_1	x_2
1	–1	–1
2	+1	–1
3	–1	+1
4	+1	+1

the value 20 pieces per mm, what provides high application quality, absence of thermal stratification and saving distinct boundaries without melting and widening of lines.

In this connection, frequency, impulse duration and lineature were identified in this research as constant values. Respectively, we could use two-factor experiment plan instead of five-factor one [29–31]. It decreased essentially the volume of conducted experiments. The following differentiated factors are noted:

– x1 – impulse capacity, %;
– x2 – marking speed, mm/s.

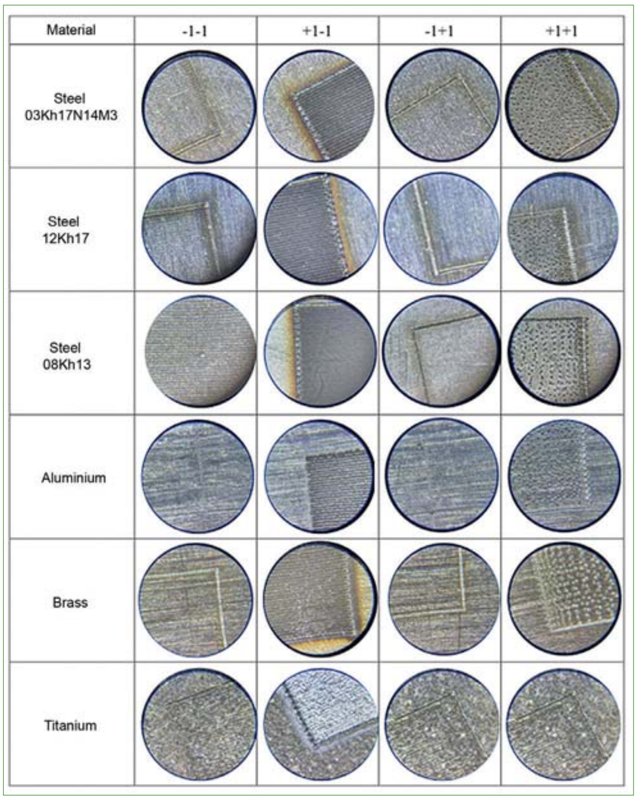

Fig. 2. The results of marking application during the two-factor experiment

The two-factor experiment plan requires only $N = 2^2 = 4$ experiments [32, 33]. The authors prepared the table of factors and their limits (**Table 2**) as well as the experiment matrix (**Table 3**).

After building a two-factor experiment, several series of laser effects were carried out for all samples (**Fig. 2**). Each combination of parameters (intensity, speed) was applied on separate surface areas, meeting the requirements of reproducibility conditions: one pass, fixed frequency (40 KHz), impulse duration (20 ns) and linear density (20 pieces).

Analysis of the results of the two-factor experiment displayed that the research within intensity range exceeding 80 % and application speed above 200 mm/s is inexpedient from the point of view both quality of forming marking and efficiency of technological process. If intensity exceeds 80 %, transition to the conditions of intensive ablation and surface melting is observed; it leads to widening of lines and decrease of geometrical accuracy of nanobar-code elements. In its turn, it finalizes in deterioration of reading ability even for visual dark trace. At the same time, at high application speed (200 mm/s), specific effect energy decreases to critically small values and does not provides sufficient local heating for forming a stable oxide layer. Use of parameters at the lower range boundary (intensity below 20 %, speed below 10 mm/s) also does not lead to improvement of marking quality. At the lowest intensity, specific effect energy is insufficient for effective absorption of laser radiation and forming a layer on metal surface, what expresses in the form of weak and non-continuous trace. When application speed is below 10 mm/s, time for code applying increases, what makes the process economically unprofitable, meaning its putting into operation in industrial scale.

Based on the established intervals (excluding defects and overheating), the new table for varying limits of factors for the two-factor experiment was built (**Table 4**). The values 20 % and 80 % were selected respectively as minimal and maximal intensity levels. The speed interval was set within the range 10–200 mm/s.

It was reveled in the previous elements that relationship between contrast and selected factors (x1 and x2) is characterized by nonlinear type, and its extremal points can be located within narrow ranges of values. Taking it into account, it was decided to conduct investigations with minimal varying step of varying parameters – 5 % and 5 mm/s. Such approach allowed not only to reveal the optimal procedures, but also to obtain the detailed map of contrast distribution (**Fig. 3**), which demonstrates the marking varying gradient. Selection

Table 4. The new factors of laser effect and their limits

Factor		Factor variation level			
		Minimal		Maximal	
Title	Designation	number	code	number	code
Impulse intensity (Factor x_1)	P, Wt	20	–1	80	+1
Marking speed (Factor x_2)	S, mm/s	10	–1	200	+1
Laser radiation frequency (Factor x_3)	F, N	const 40			
Impulse duration (Factor x_4)	τ, ns	const 20			
Number of lines per mm (Factor x_5)	μ, pieces	const 20			

of small step was based on necessity to obtain the detailed information for consequent building of mathematical model and development of managing system on laser marking parameters [18].

To provide quantitative evaluation of marking contrast, digital data processing was carried out [34, 35]. Each matrix module, which corresponds to determined combination of marking intensity and speed, was analyzed via special program for measurement of coloured parameters. Each module was identified with average colour value according to RGB system; it allowed to step up from visual interpretation to objective data and to build a mathematical model.

To determine contrast of each module, the following derived formula was used:

$$C = \left(1 - \frac{R+G+B}{765}\right) \times 100\% \qquad (1)$$

where R, G, B – average intensity values of coloured channels,

765 – maximal sum, which corresponds to white colour.

The obtained data allowed to build the tables of contrast distribution (**Table 5**, **Table 6**) and to reveal the optimal interval of technological parameters.

RGB system is standard for digital processing of images, which were obtained via microscopy and from digital cameras [10, 34, 36]. The formula operates correctly in the cases, when marking has black tones and coloured channels are close with each other (R≈G≈B). It corresponds to the conditions of experiment conducting, because achromatic

Table 5. Fragment of the matrix with RGB identified for each module, for the sample of steel

	P = 20 %	P = 25 %	...	P = 80 %
υ = 10 mm/s	122, 120, 105	94, 81, 63	...	52, 45, 41
	P = 20 %	P = 25 %	...	P = 80 %
υ = 15 mm/s	88, 91, 90	90, 81, 68	...	68, 57, 53
...	...	...	...	...
υ = 200 mm/s	229, 228, 224	236, 227, 210	...	127, 106, 77

Table 6. Contrast calculation via the formula (1)

	P = 20 %	P = 25 %	...	P = 80 %
υ = 10 mm/s	55 %	69 %	...	82 %
υ = 15 mm/s	65 %	69 %	...	80 %
...	...	...	...	...
υ = 200 mm/s	11 %	12 %	...	59 %

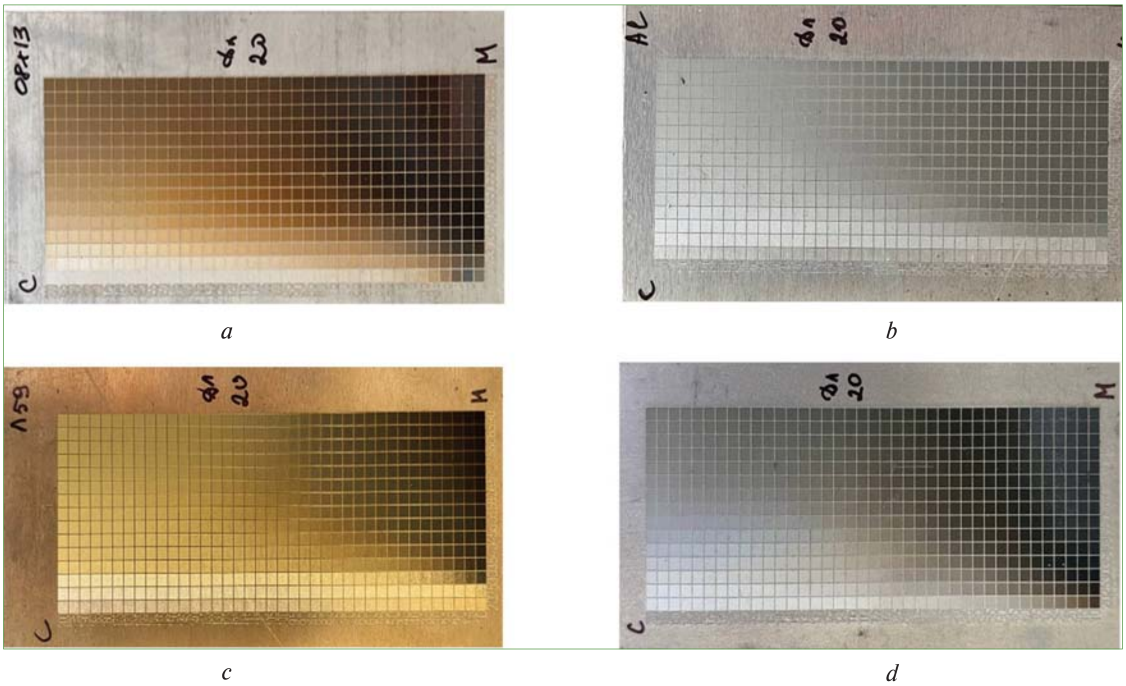

Fig. 3. Example of matrix application on the samples: *a*) steel 08Kh13, *b*) aluminium; *c*) brass; d) titanium

(colorless) marking is forming for all examined conditions, and contrast is determined by the value of surface dimming.

Based on the obtained table with experimental data, the contrast matrix was built (**Fig. 4**). This form of data interpretation allows evaluate obviously contrast distribution along the whole area of parameters and to reveal the zone of optimal conditions.

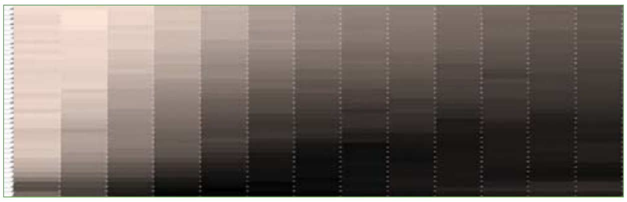

Fig. 4. The contrast matrix in Excel

To provide more detailed analysis of relationship between contrast (from one side) and intensity and speed (from other side), the 3D response surface model (Python software environment) was developed (**Fig. 5**). This model was built on the base of the massif of experimental data, it provides visualization of contrast as a function of two variables. Such approach allows not only to evaluate the effect of parameters with high quality, but also to determine the peak of optimal zone and to use the model for prediction of the results for intermediate values of the conditions.

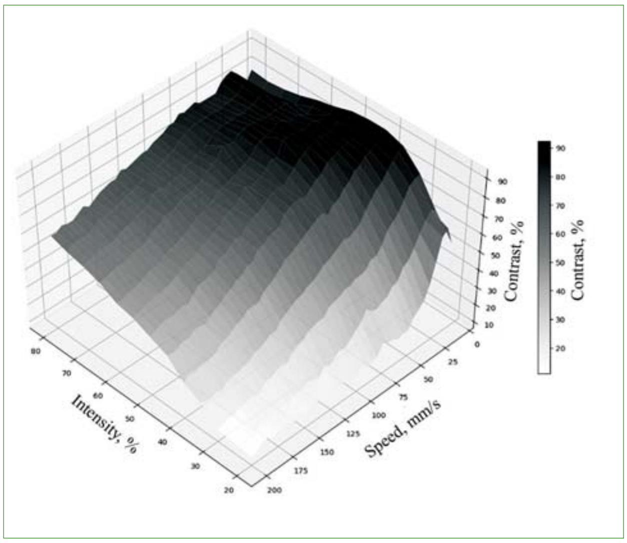

Fig. 5. The response surface model using Python software environment

Data analysis displayed that maximal contrast (93 %) is achieved within intensity range 35–50 % and speed range 10–20 mm/s. When speed increasing above 50 mm/s or intensity decrease below 30 %, contrast drops below 80 %. In these conditions, laser radiation energy is insufficient for forming dense oxide layer, what can lead to deterioration of observability of code modules. In the same way, extremely high intensity (above 60 %) and low speed (below 10 mm/s) causes appearance of overheating signs: melting, deformation, roughness increase [37]. Thus, the optimal interval of NBC forming for steel 08Kh13 is determined within the range P = 40–45 % and υ = 15–20 mm/s.

Based on the experimental data, two regression models describing forming of contrast NBC marking for steel 08Kh13 were built.

1. The optimal zone for dark modules (black marking) is determined within intensity range 40–45 % and speed range 10–20 mm/s. Let's build the table (**Table 7**) for two-factor experiment in the selected range.

Table 7. Two-factor experiment in the selected range for high contrast

No.	P, %	V, mm/s	X_1	X_2	C, %
1	40	10	–1	–1	90
2	45	10	+1	–1	93
3	40	20	–1	+1	99
4	45	30	+1	+1	91

2. The optimal zone for low contrast is determined within intensity range 20–30 % and speed range 150–200 mm/s. So, the conditions for low contrast are presented in the **Table 8**.

Table 8. Two-factor experiment in the selected range for low contrast

No.	P, %	V, mm/s	X_1	X_2	C, %
1	20	150	–1	–1	14
2	305	150	+1	-1	22
3	20	200	–1	+1	11
4	30	200	+1	+1	13

Let's use the linear model:

$$C = b_0 + b_1 x_1 + b_2 x_2 , \qquad (2)$$

where C – contrast,

x_1 – coding intensity;

x_2 – coding speed,

b_0, b_1, b_2 – coefficients which were determined during experiment.

Free term b_0 (3):

$$b_i = \frac{1}{N} \sum_{i=1} y_i x_{ij} \qquad (3)$$

where $N = 4$ – total number of experiments,

y_i – response value in the i-th experiment,

x_{ij} – value of the j-th factor in the i-th experiment.

The final model for high and low contrast according to the formula (2) looks like:

$C_{dark} = 90.5 + 1.5x_1 – 1.0x_2$

$C_{light} = 15 + 2.5x_1 – 3.0x_2$

The formulas display that intensity has more strong effect on marking contrast in the case of dark contrast. As for light contrast, speed has decisive effect.

The developed regression models allow conducting analysis of features of the effect of each of the examined laser parameters on contrast degree for obtained nanobar-codes [4, 33].

The obtained data were confirmed by the series of real experiments. Fragments of a nanobar-code were formed according to the determined optimal interval. Microscope snapshots were made for detailed analysis of the surface and quality of code forming (**Fig. 6**).

Experimental researches, that have been carried out with various metals, confirmed efficiency of the developed

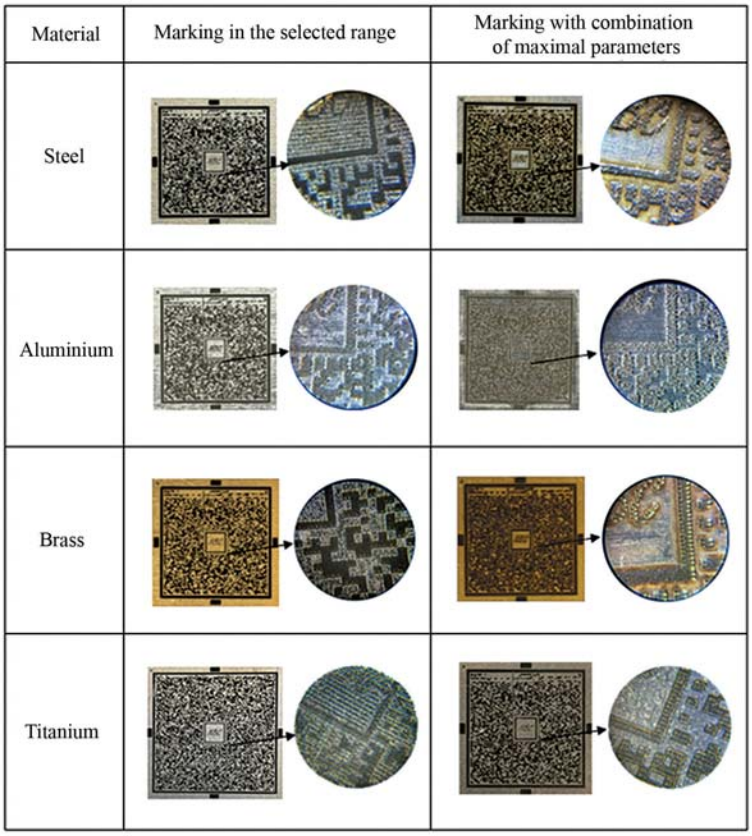

Fig. 6. Pictures of nanobar-code fragments on the surface

and suggested method of nanobar-code forming. Microscope snapshots demonstrate qualitative difference between marking executed according to the proposed technique and marking applied with combination of maximal laser parameters. In the first case we observe distinct and well-expressed boundaries of modules, while in the second case – fuzzy contours and violation of elements geometry, what deteriorates information capacity and code readability.

Conclusion

Based on the results of conducted work, the following conclusions can be done.

1. The technique of searching the optimal parameters of forming ultra-dense nanobar-code was realized on the example of steel 08Kh13. 507 combinations of laser conditions were analyzed in order to reveal the maximal contrast zone.

2. The research displays that contrast of marking on steel 08Kh13 depends maximally on intensity and speed of marking application. Maximal contrast (93 %) is achieved at intensity 40–45 % and speed 10–20 mm/s. As for other steels 12Kh17 and 03Kh17M3, the optimal interval is the same. Aluminium is characterized by intensity 60–90 % and speed 10–30 mm/s intervals, brass has optimal values of intensity and speed within the ranges 40–60 % and 10–20 mm/s, while titanium displays maximal contrast for intensity 30–35 % and speed 10–25 mm/s.

3. The scheme for application of dark and light code elements for opposite laser parameters is suggested. This approach creates maximal optical contrast, similar to printed code on paper and provides high readability.

4. The analysis displayed that speed increase up to 20 mm/s without losing marking quality is possible with saving high contrast, what decreases time for NBC application.

5. The visual instruments – the contrast matrix and 3D model – were developed for illustrative selection of procedures.

Input of the authors:

Pryakhin E. I., Dr. Eng. – conceptual development of the technology;

Dranova A. Yu., Post-graduate – practical realization of the technology, collection and processing of the experimental data.

REFERENCES

1. Vasilyeva M. V., Vasilyeva M. A. The role of technology for goods traffic monitoring in providing the state safety. *Obrazovanie i pravo*. 2021. No. 8. pp. 124–130. DOI: 10.24412/2076-1503-2021-8-124-130.
2. Nadvotskaya V. V., Yengibaryan E. A. Problems of putting into practice of the information system for product marking. *Polzunovskiy almanakh*. 2022. No. 4-1. pp. 62–65.
3. Sheremet D. A., Silaev A. A., Nosenko V. A. The remedies of identification and observability of products presented in the Russian market for manufacture of large diameter pipes. *Inzhenernyi vestnik Dona*. 2024. No. 4 (112). pp. 156–167.
4. Vybornov O. A. Laser in metrology and materials processing. *Simvol nauki: mezhdunarodnyi nauchnyi zhurnal*. 2023. No. 10-1. pp. 23–24.
5. Nikishova A. V., Glybina E. M., Umnitsyn M. Yu. Neurocryptographic protection of information. *NBI tekhnologii*. 2022. Vol. 16. No. 2. pp. 17–20. DOI: 10.15688/NBIT.jvolsu.2022.2.3.

6. Polukhin A. Yu., Bondarev A. D., Kaigorodova E. R. et al. Control and measuring scanning system for bar-codes from printed circuit boards during production process. *Inzhenerhyi vestnik Dona*. 2022. No. 1 (85). pp. 176–183.
7. Fomin A. V., Glushchenko A. I., Poleshchenko D. A. Use of laser marking devices for solving the problem of aditional marking application on steel billet. *Metallurg*. 2020. No. 1. pp. 46–50.
8. Pryakhin E. I., Pribytkova D. A. Development and application of a complex polymer coating to ensure high corrosion resistance of the outer surface of steel pipes of urban heating networks. *CIS Iron and Steel Review*. 2025. Vol. 29. pp. 97–101.
9. Efimov A. E., Uspenskaya V. D., Motrich A. A. Improving the quality of processing articles made of low-alloy ferrite-pearlite steels using concentrated laser emission. *Chernye metally*. 2024. No. 9. pp. 77–81.
10. Petkova A. P., Ganzulenko O. Yu. Laser marking of non-ferrous metal and alloy products using ultradense barcodes: process features. *Tsvetnye metally*. 2022. No. 7. pp. 92–97.
11. Syrkov A. G., Prokopchuk N. R., Vorobiev A. G., Brichkin V. N. Academician N. S. Kurnakov as the founder of physico-chemical analysis – the scientific base for the development of new metal alloys and materials. *Tsvetnye metally*. 2021. No. 1. pp. 77–83.
12. Kuzmin M. I., Ponomareva A. I., Gerasimov R. V. An approach to adapting management of the holes fund with mounting an electric vane pump. *Neftyanoe khozyaistvo*. 2025. No. 7. pp. 130–134. DOI: 10.24887/0028-2448-2025-7-130-134.
13. Safonov S. A. Statistical analysis of violation detection within the range of a linear regression model. *Dvoinye tekhnologii*. 2023. No. 3 (104). pp. 20–24.
14. Gornyi S. G., Zakharenko E. A., Klassen N. V. Laser forming and influence of laser radiation on the main parameters of baecodes. *Fizika i khimiya obrabotki materialov*. 2021. No. 6. pp. 61–70. DOI: 10.30791/0015-3214-2021-6-71-70.
15. Gorny S. G., Zakharenko E. A., Klassen N. V., Kolobov Y. R., Ligachev A. E., Pryakhin E. I., Odintsova G. V. Laser formation and influence of laser radiation on basic characteristics of barcodes. *Inorganic Materials: Applied Research*. 2022. Vol. 13. No. 3. pp. 879–886. DOI: 10.1134/S2075113322030121.
16. Moldovanov A. A., Korochkin L. S., Shmakov M. S. Forming of additional protection for matrix barcodes. *Trudy BGTU. Seriya 4: Print- i mediatekhnologii*. 2021. No. 2 (49). pp. 62–68. DOI: 10.52065/2520-6729-2021-249-2-62-68.
17. Pryakhin E. I., Dranova A. Yu. Features of modular structure forming for 2D codes with high density via direct laser marking on metal. *Dizain. Materialy. Tekhnologii*. 2024. No. 2 (74). pp. 184–189. DOI: 10.46418/1990-8997_2024_2(74)_184_189.
18. Yugov V. I. Efficient direction of laser technology development – creation of laser complexes. *Glavnyi mekhanik*. 2020. No. 1. pp. 38–50.
19. Petkova A. P., Ganzulenko O. Yu. Features of colour ultradense multidimensional nanobarcodes created on the surface of items made of non-ferrous metals and their alloys. *Tsvetnye metally*. 2023. No. 8. pp. 19–25.
20. Konchus D. A., Sivenkov A. V., Pryalhin E. I. Features of laser marking of metallic products. *Informatsionno-tekhnologicheskiy vestnik*. 2020. No. 1 (23). pp. 157–164.
21. Mikhailov A. V. , Piirainen V. Yu., Bobrova E. M., Smirnov A. I. Analysis of prospects for using peat amendments for damaged soil reklamation. *Gornaya promyshlennost Rossii*. 2025. No. 2. pp. 124–130. DOI: 10.30686/1609-9192-2025-2-124-130.
22. Spirin M. S., Izoriya D. A. Effect of laser radiation on chemical transformations in polymer materials. *Moya professionalnaya karyera*. 2025. Vol. 1. No. 69. pp. 67–75.
23. Pisareva O. A., Rukhadze D. M. Software and standardization in the field of laser scanning technologies. *Modern Science*. 2022. No. 4-2. pp. 347–351.
24. Vologzhanina S. A., Ermakov B. S., Ernakov S. B., Khuznakhmetov R. M. Relationship between operating conditions and the emergence of nano- and ultradispersed grain boundary defects in weld joints. *Tsvetnye metally*. 2023. No. 8. pp. 80–85.
25. Litvinenko V. S., Petrov V. I., Vasilevskaya D. V., Yakovenko A. V., Naumov I. A., Ratnikov A. M. Evaluation of the state role in management of mineral resources. *Zapiski Gornogo instituta*. 2023. No. 259. pp. 95–111. DOI: 10.31897/PMI.2022.100.
26. Shakhnazarov K. Yu., Rafikov A. R. Influence of the conditions of hardning heat treatment on crack propagation resistabnce for stamping steel 5Kh2SMF. *Frontier Materials & Technologies*. 2025. No. 2. pp. 13–28. DOI: 10.18323/2782-4039-2025-2-72-0.
27. Amyaga D. V., Gornyi S. G., Volohzhanina S. A. The method of surface concave marking for steel products using impulse infrared fiber laser with intensity 50 Wt. *Tekhnologiya metallov*. 2020. No. 6. pp. 27–33. DOI: 10.31044/1684-2499-2020-0-6-27-33.
28. Kozhakhmetova A. M. Physics of lasers: types, properties, operating principles and application. *Vestnik nauki*. 2024. Vol. 3. No. 12 (81). pp. 1582–1590.
29. Mustafin M. G., Zubov A. V., Vasilyev G. V. Evaluation technique for deformation process during monitoring of engineering constructions. *Gorny unformatsionno-analiticheskiy byulleten*. 2025. No. 8. pp. 92–113. DOI: 10.25018/0236_1493_2025_8_0_92.
30. Litvinova T., Gerasev S., Sergeev V., Lidanovskiy E. Rare Earth Metal Ion-Associates in Ln^{3+}—CO_3^{2-}—H_2O System. *Metals*. 2025. Vol. 15. pp. 239. DOI: 10.3390/met15030239.
31. Povarov V. G., Cheremisina O. V., Alferova D. A., Fedorov A. T. Determination of the Activity Coefficients of Components in a Di-2-ethylhexylphosphoric Acid–n-Hexane Binary System Using Gas Chromatography. *Chemistry*. 2025. Vol. 7. pp. 92. DOI: 10.3390/chemistry7030092.
32. Litvinova T. E., Vasilyev V. V., Tuleshov N. V. Effect of sulfate anion on the decomposition rate of alkaline aluminate solutions. *Tsvetnye metally*. 2025. No. 7. pp. 39–44.
33. Zharkov A. M., Peskov D. V., Martynov A. V. Identification of Hydrocarbon Accumulation Zones on Ancient Platforms in the Northern Part of Eurasian Lithospheric Plate. *International Journal of Engineering, Transactions B: Applications*. 2025. Vol. 38. No. 11. pp. 2713–2727. DOI: 10.5829/ije.2025.38.11b.19.
34. Garbar E. A.,Logunova O. S., Narkevich M. Yu. Sdudies on workability of processing algorithms for surface of metallic sheet materials. *Matematicheskoe i programmnoe obespechenie sistem v promyshlennoy i sotsialnoy sferakh*. 2023. Vol. 11. No. 1. pp. 31–36.
35. Shakhnazarov K. Yu., Vologzhanina S. A., Khuznakhmetov R. M. Explanation of structure forming anomalies and physico-mechanical properties of steels and alloys. *Informatsionno-tekhnologicheskiy vestnik*. 2023. No. 1 (35). pp. 196–209.
36. Pivovarov A. D., Usynina E. V., Sinev D. A. Direct laser thermomechanical recording on titanium films for creation of a screened image. *Nauchno-tekhnicheskiy vestnik informatsionnykh tekhnologiy, mekhaniki i optiki*. 2025. Vol. 25. No. 1. pp. 23–32. DOI: 10.17586/2226-1494-2025-25-1-23-32.
37. Moldovanov A. A., Korochkin L. S., Shmakov M. S. Software module for coding and modification of barcodes. *Trudy BGTU. Seriya 4: Print- i mediatekhnologii*. 2020. No. 2 (237). pp. 5–10.